

## Handling of Bulk Solids in a Marine Environment from Seabed to Shore

Schott, D.L.; de Hoog, E.; van Wijk, J.M.; Helmons, R.L.J.

**DOI**

[10.1007/978-3-031-59060-3\\_4](https://doi.org/10.1007/978-3-031-59060-3_4)

**Publication date**

2024

**Document Version**

Final published version

**Published in**

Deep-Sea Mining and the Water Column

**Citation (APA)**

Schott, D. L., de Hoog, E., van Wijk, J. M., & Helmons, R. L. J. (2024). Handling of Bulk Solids in a Marine Environment from Seabed to Shore. In R. Sharma (Ed.), *Deep-Sea Mining and the Water Column: Advances, Monitoring and Related Issues* (pp. 91-127). Springer. [https://doi.org/10.1007/978-3-031-59060-3\\_4](https://doi.org/10.1007/978-3-031-59060-3_4)

**Important note**

To cite this publication, please use the final published version (if applicable).  
Please check the document version above.

**Copyright**

Other than for strictly personal use, it is not permitted to download, forward or distribute the text or part of it, without the consent of the author(s) and/or copyright holder(s), unless the work is under an open content license such as Creative Commons.

**Takedown policy**

Please contact us and provide details if you believe this document breaches copyrights.  
We will remove access to the work immediately and investigate your claim.

***Green Open Access added to TU Delft Institutional Repository***

***'You share, we take care!' - Taverne project***

**<https://www.openaccess.nl/en/you-share-we-take-care>**

Otherwise as indicated in the copyright section: the publisher is the copyright holder of this work and the author uses the Dutch legislation to make this work public.

# Chapter 4

## Handling of Bulk Solids in a Marine Environment, from Seabed to Shore



Dingena Schott, Edwin de Hoog, Jort van Wijk, and Rudy Helmons

**Abstract** In this chapter, the work that is being done in relation to machine-cargo interactions relevant to deep-sea mining is elaborated. To ensure safe and efficient operations across the entire mining value chain, it is important to be aware of the implications of certain design and process decisions. An overview of mechanisms influencing the mechanical response of the bulk materials and the main effects leading to (mechanical) degradation of the ore, e.g., fragmentation, abrasion, is presented. Although the concepts are applicable to each of the deep-sea deposits, our focus is on polymetallic nodules in a riser-based concept.

Results are discussed of experiments in which nodules are fragmented due to particle-particle collisions and collisions with different handling equipment, such as the seabed harvester, riser pipe, pump impeller, pipe bends, etc. Next to fragmentation, degradation due to abrasion occurs due to particles rolling, sliding, and collid-

---

D. Schott (✉)

Department of Maritime and Transport Technology, Faculty of Mechanical Engineering,  
Delft University of Technology, Delft, The Netherlands  
e-mail: [D.L.Schott@tudelft.nl](mailto:D.L.Schott@tudelft.nl)

E. de Hoog

Department of Maritime and Transport Technology, Faculty of Mechanical Engineering,  
Delft University of Technology, Delft, The Netherlands

Royal IHC, Kinderdijk, The Netherlands

e-mail: [e.dehoog@royalihc.com](mailto:e.dehoog@royalihc.com)

J. van Wijk

Independent Consultant Hydraulic Transport System Engineering,  
Slidrecht, The Netherlands

Geotechnical Advisory Services, IQIP, Slidrecht, The Netherlands

R. Helmons

Department of Maritime and Transport Technology, Faculty of Mechanical Engineering, Delft  
University of Technology, Delft, The Netherlands

Institute of Geoscience and Petroleum, Norwegian University of Science and Technology  
(NTNU), Trondheim, Norway

e-mail: [R.L.J.Helmons@tudelft.nl](mailto:R.L.J.Helmons@tudelft.nl)

ing with each other, resulting in the generation of nodule fines. Based on the same set of nodules, mechanical bulk properties of dry and wet nodules are studied. The obtained results provide relevant insights for the design of the nodules handling equipment. Furthermore, modelling approaches applied to other fragile bulk materials where the breakage and generation of fines play an important role are outlined. It is described how these modelling approaches can assist in the design of handling equipment, and recommendations are given for next steps to further optimize their design.

**Keywords** Polymetallic nodules · Degradation · Fragmentation · Friction

## Abbreviations

|     |                            |
|-----|----------------------------|
| BPM | Bonded particle model      |
| DEM | Discrete element method    |
| FBM | Fast-breakage model        |
| MSV | Mining support vessel      |
| PmN | Polymetallic nodules       |
| PRM | Particle replacement model |

## 1 Introduction and Overview of Handling Steps

Deep sea mining has emerged as a promising solution to meet the growing demand for critical metals and minerals. Figure 4.1 shows a schematic of the steps involved in transport from seabed to shore, where the manganese or polymetallic (PmN) nodules will be processed. The nodules that will be picked up from the seabed, subsequently handled by the seabed harvester, and transported vertically to the mining support vessel (MSV). Various vertical transport concepts exist, such as hydraulic, airlift and skip-lift concepts. At the MSV, handling of bulk materials takes place optionally with processing steps such as dewatering and filtering of fines. The excess of water and sediments is to be discharged subsea.

While the MSVs work far offshore, the material will be transhipped to vessels that operate between the MSV and a location on shore. Once the material is onshore it might be first handled and stored at a bulk storage terminal before being transported to the nodules processing plant. At this moment, such a supply chain is not yet practically established, although a first trial focussing on the first steps in Fig. 4.1 resulted in the collection from the seabed to the MSV of about 4500 tons PmN (Allseas, 2022). It goes without saying that for an optimal, sustainable and energy-efficient supply chain, the focus should not only be on developing the initial steps, but efforts are required to develop the logistics system including all the handling steps from seabed to shore.



**Fig. 4.1** Deep-sea mining value chain and bulk handling steps from MSV to processing facility

Starting from the right side in Fig. 4.1, the demands of the polymetallic nodule extraction plant in terms of (1) required material quality/properties (form, size and distribution) depending on the extraction processes and (2) infeed capacity are crucial to design the logistic system. These demands are posed to the previous steps upstream in Fig. 4.1.

For the mining capacity in general, if the processing capacity is too low relative to the mining capacity, there may be a bottleneck in the supply chain as the raw material accumulates and waiting times for processing increase. This can lead to increased costs and delays in the supply chain. On the other hand, if the processing capacity is too high relative to the mining capacity, the supply chain may be underutilized, and there may be excess capacity in downstream operations, leading to wasted resources and increased costs.

For the material quality, the requirement depends on the type of extraction process, which can be divided into two main streams (Monhemius, 1980), pyro-hydro-metallurgical routes and hydrometallurgical processes, where drying of the wet nodules is not necessary. Randhawa et al. (2016) describe different processing routes in detail and indicate crushing and grinding steps for all processes. The ideal material properties for the extraction processes and state of the material (wet or dry) from downstream should be considered in the design of the logistics systems and its handling components. In every handling step, due to the interaction of the material with the equipment, breakage of the material might happen.

It is important to reduce the breakage of nodules during the handling steps from seabed to shore in deep-sea mining operations for several reasons. Firstly, nodules are relatively fragile and can easily break apart during the handling steps and transport. This can result in a significant loss of valuable material, reducing the overall yield of the operation and potentially impacting its economic viability. Secondly, the broken nodules can generate fine particles or dust, which can be difficult to handle and may cause problems during processing or transportation or are economically unattractive to separate at the MSV. Fine particles can cause problems such as clogging of pipes and increased wear and tear on machinery and can even be hazardous to workers' health, if inhaled. Lastly, broken nodules can also have a

negative impact on the marine environment as the fine particles generated by breakage can get dispersed over a wider area, potentially affecting marine ecosystems and biodiversity.

In this chapter, we will address the breakage and material properties in the context of material equipment interactions during handling from seabed to shore. In Sect. 2, we address degradation mechanisms in relation to hydraulic transport processes and provide quantitative results of laboratory tests. In Sect. 3, the mechanical response of the bulk and its machine cargo interactions will be reported. Issues related to particle breakage, degradation and the creation of fines are also common in the biomass handling field. Hence, Sect. 4 will cover the experimental and numerical methods used in research on the handling of biomass pellets specifically. Section 5 concludes this chapter by summarizing the key findings and discussing their implications for the outlook of deep-sea mining.

## **2 Fragmentation of Polymetallic Nodules Due to Impacts from Seafloor to MSV**

From the bulk processing and mining industries, a method is available to quantify and measure the wear or degradation of minerals and ores (Beekman et al., 2002). However, in the context of deep-sea mining, we first need to approach this problem from the viewpoint of hydraulic transportation as it is the most considered transportation option among deep-sea mining concepts. Since the reduction of the size of the nodules and generation of nodule dust determine the design choices, of processing equipment on the MSV to a large extent, the degradation mechanisms associated with the transport processes need to be evaluated to enable further quantification.

This section gives an overview of work done to assess the magnitude of polymetallic nodule degradation during deep-sea mining. First, we explain degradation mechanisms and relate them to hydraulic transport processes in typical pipeline concepts. Second, we quantify a bandwidth of degradation rates and effects, based on laboratory tests. Each test is dedicated to investigating one specific degradation mechanism, and the results are summarized.

### ***2.1 Degradation Mechanisms***

Vertical transport of polymetallic nodules to the sea surface can be realized by a number of different technologies, of which mechanical lifting, airlifting and centrifugal pump-based hydraulic transport are the most prominent candidates (Ma, 2019). Airlift technology is proven on full-scale, however, controllability and sufficiently high production rates are a challenge (Ma et al., 2017). Hydraulic transport, by means of a riser system with centrifugal pump booster stations, has the

potential of stable, large production rates, however at the cost of more technology components being below sea level (van Wijk, 2016).

The actual particle size distribution (PSD) of the mixture leaving the riser is a key design parameter for the processing equipment (both on the mining support vessel and on land). The degradation of nodules to particle size fractions smaller than those that can be effectively recovered during the processing of the slurry on board the mining vessel means loss of valuable ore and aggravates the environmental pressures related to the discharge of fines in the marine environment. It is, therefore, important to have predictive models and data that allow for quantification of nodule degradation.

Particle degradation occurs in all multiphase flows involving solids in a carrier fluid. Depending on the force, magnitude and direction, the modes of degradation are attrition, fragmentation, abrasion, and chipping (see Fig. 4.2) (Laarhoven et al., 2012).

The degradation process is closely linked to the hydraulic transport process. The degradation process is complex, involving both impact fracturing as well as abrasion due to friction. Impact fracturing mainly occurs in centrifugal pumps, while abrasion mainly occurs in the pipeline (Worster & Denny, 1955). Bergh and Grima (2006) have reported on degradation experiments with limestone and coarse gravel in a test circuit and on the degradation of quartz, sand and rock salt during dredging. These four material types showed both impact fracturing by the centrifugal pump and abrasion due to the horizontal hydraulic transport, but the relative contribution of one mechanism over the other differs between the cases. Especially rock salt and coarse gravel were influenced by impact fracturing occurring in the centrifugal pump.

Yamazaki and Sharma (2001) experimentally studied the degradation of subsea sediments from the CCZ zone. They used a small-scale circulating flow loop, including one pump and a few metres of pipeline, operated for 30 min. The resulting PSDs point at the production of significant amounts of fines. The maximum sediment diameter in their test reduced from about 200 µm to 50 µm. This indicates that the already fine seabed sediment will become even finer upon transport. Yamazaki et al. (1991) show the PSD of abraded nodules after passing through the pump and

**Fig. 4.2** Particle degradation depends on the applied force and its direction based on terminology by Beekman et al. (2002). (Figure from: Laarhoven et al. (2012), Copyright Elsevier 2012, reprinted with permission)

| Magnitude                     | Direction                                                                                            |                                                                                                 |
|-------------------------------|------------------------------------------------------------------------------------------------------|-------------------------------------------------------------------------------------------------|
|                               | Normal                                                                                               | Tangential                                                                                      |
| Low<br>(wear dominant)        | Attrition<br>     | Abrasion<br> |
| High<br>(fracturing dominant) | Fragmentation<br> | Chipping<br> |

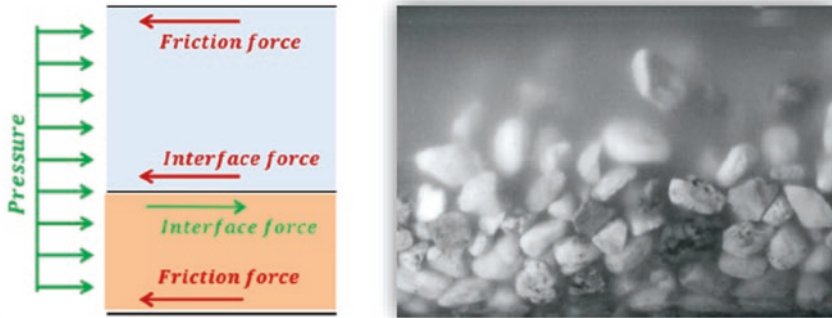


**Fig. 4.3** A sliding bed of particles with shear layer and its associated force balance. This situation typically occurs in the flexible jumper hose. (From: de Hoog (2016), reprinted with permission)

riser pipe. Unfortunately, no initial PSD is known, so no conclusions about degradation rates could be drawn. A closer look at the individual transport processes is necessary to quantify the relative contributions of the different degradation mechanisms.

The slurry first enters the SMT pump, where it is subjected to mainly impact fracturing in the pump. The lazy-wave configuration of the jumper hose will mainly result in heterogeneous hydraulic transport. When particles are too large to be suspended by turbulence, they will form a sliding bed layer at the bottom of the pipe (Vlasak et al., 2013) (Ravelet et al., 2013) (de Hoog et al., 2017; Spelay et al., 2016) (see Fig. 4.3). Such a sliding bed of nodules and sediments is predominant in the inclined and horizontal parts, above which a shear layer will develop. This sliding bed transport regime will mainly cause attrition and abrasion of the nodules by sliding over the pipeline bottom, by Coulombic friction. In addition, attrition and abrasion are also caused by particle layers sliding and tumbling over each other in the shear zone.

In the riser segments, there are two mechanisms involved. The first is particle abrasion by particles sliding along the riser segments. The second mechanism is degradation by particle interaction in the riser segments. Different particle fractions have different transport velocities (van Wijk et al., 2016), and their relative velocities give rise to collisions and probably mild impact fracturing or attrition. Particle–wall interaction will have velocities in the order of the pipeline bulk velocity, that is several meters per second. Particle–particle interaction will have velocities in the order of the hindered settling velocity, which is an order of magnitude smaller than the bulk velocity (van Wijk, 2016). In the case of vertical transport with centrifugal pump booster stations, the bends and pumps in the booster give rise to degradation by impact fracturing.

Summarized, Table 4.1 provides an overview of all degradation mechanisms expected during hydraulic transport.

**Table 4.1** Main transport mechanisms and their associated degradation mechanisms

| VTS component   | Transport mechanism                                | Degradation mechanism          |
|-----------------|----------------------------------------------------|--------------------------------|
| Jumper          | Heterogeneous flow, shear layer                    | Abrasion by friction (sliding) |
| Riser           | Pseudo-homogeneous flow                            | Abrasion with riser wall       |
| Riser           | Pseudo-homogeneous flow                            | Inter-particle collision       |
| Pumps, boosters | Highly turbulent, many machine–nodule interactions | Impact fragmentation           |

## 2.2 Fragmentation of Nodules Due to Impact

In Sect. 2.1, we discussed the different transport processes occurring in the SMT and VTS, and we related these transport processes to degradation mechanisms. The next step is the quantification of the different degradation mechanisms. In this section, we first investigate impact fragmentation.

The impact fracturing of polymetallic nodules in centrifugal pumps shows a complex interplay between particles and the pump. The role of centrifugal pumps in the degradation of coal was investigated in the 1980s (Shook et al., 1979; Gilles et al., 1982). Despite the many similarities with hydraulic transport for deep-sea mining, the work on coal transport is too specifically dedicated to horizontal transport under atmospheric conditions to be representative and of direct use for vertical transport from the deep sea.

Especially the very large ambient pressure in the deep sea is an important difference that needed further investigation. To this end, a special centrifugal pump test setup was constructed in the high-pressure basin at the Royal Netherlands Institute for Sea Research, NIOZ, The Netherlands (van Wijk et al., 2019).

A polymetallic nodule is formed as various minerals precipitate from the surrounding water on a nucleus, typically, an older nodule, shark tooth, volcanic rock or shell. As the nodule grows, a layered internal structure is formed, commonly with local sediments trapped between the layers.

These sediments compromise the strength of the nodule and cause breakage typically to occur along these weak points. Larger nodules consist of more layers and weak points; therefore, they are usually weaker than smaller nodules as is evident by compressive strength tests (Dreiseitl, 2017) (van Wijk & de Hoog, 2020). Some nodules are an agglomeration of smaller nodules that grew together over time.

The test setup at the NIOZ was constructed to accommodate the largest nodules that can reasonably be expected during normal VTS operation, for example  $d/D_i \approx 3/5$ . From a sample of UK and Belgian nodules from the CCZ (fully saturated with fresh water at 5°), the 16–32 mm fragments were chosen to fit the test setup. In contrast to the rounded appearance of intact nodules, these fragments were mostly of irregular and angular shape. The fragments have been formed due to the disintegration of intact nodules along the internal weakest parts. The fragments themselves could therefore be relatively strong compared to the original intact nodules.

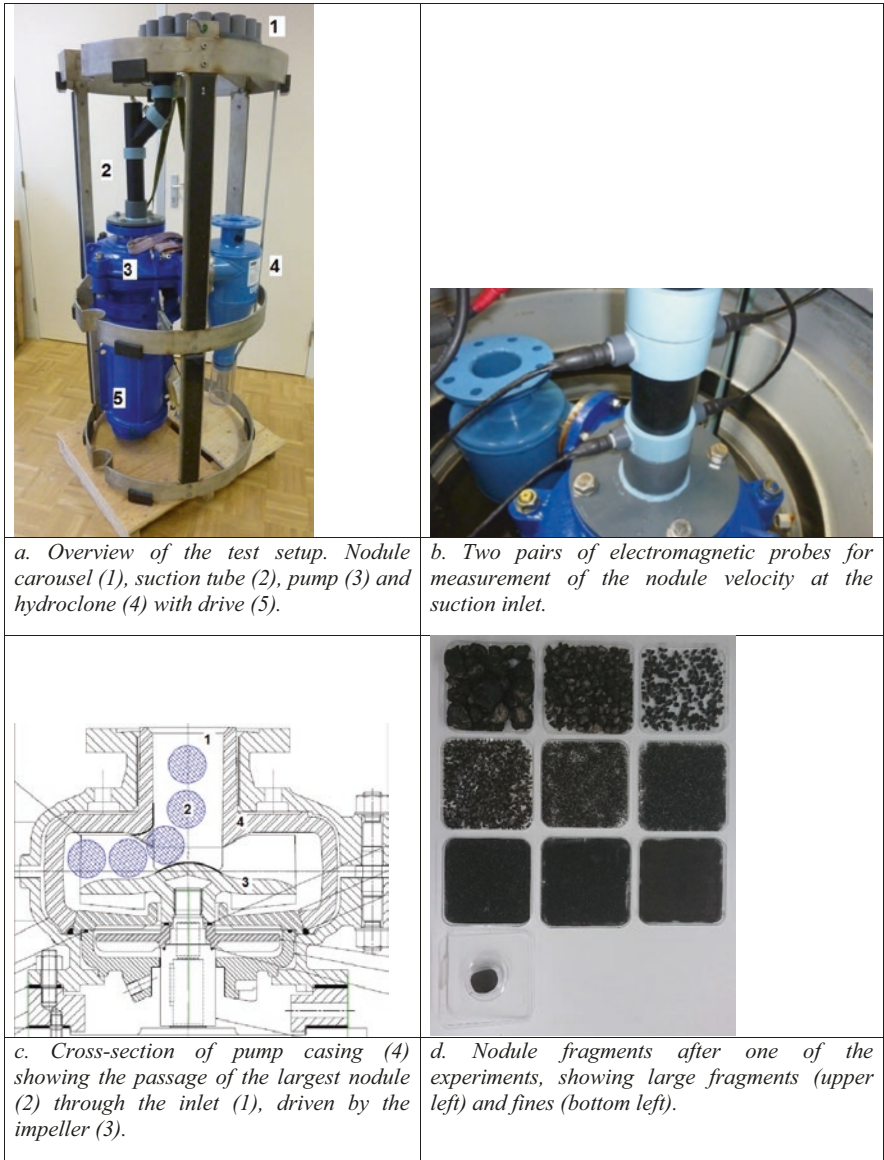
The test setup is depicted in Fig. 4.4. After the passage of the pump, the nodule enters a hydro cyclone where the fine grit and coarser fragments are separated to enable detailed analysis of the particle size distributions. In the tests, nodules were passed through the setup applying different pump velocities (750, 1200 and 1800 rpm, respectively) and ambient pressures of 5, 95, 189, 283, 378 and 500 bar. Nodules and nodule grit recovered after each test run were wet-sieved over a series of sieves with logarithmically increasing mesh size from 0.063 to 32.00 mm. The retained fractions were freeze-dried and weighed. Fractions below  $d < 63 \mu\text{m}$  were measured with a laser particle analyzer. Next to single runs carried out under one particular combination of pump speed and pressure, tests were carried out simulating the passage of nodules through the full series of pumps of the VTS positioned at different water depths. While running the pump at different velocities, nodules and nodule grit were passed multiple times through the pump, consecutively at 500, 378, 283, 189, 95 and 5 bar. It should be noted that the fine-grained material retrieved from the water contained abundant chips of blue paint abraded from the interior of the hydrocyclone, providing evidence of abrasion occurring within the hydrocyclone, adding fine-grained material to the fractions produced in the pump.

Figure 4.5 shows the particle size distributions produced at different ambient pressures but similar pump speeds of 750 and 1800 rpm, respectively. This figure shows that the distribution of material after impact fracturing is hardly influenced by the ambient pressure. The results at 1800 rpm show a similar trend, but far more material has fractured and moved into smaller size classes. The single passage experiments show hardly any influence of the high ambient pressure conditions and a large influence of nodule velocity or impeller speed. The sequential experiments, in which the same batch of nodules was pumped at decreasing ambient pressure, with six stages in total, are therefore not expected to be influenced by the changing ambient pressure. Pump speed however does have a large influence on nodule degradation, so for the sequential experiments, more degradation is expected at higher pump speeds as well. Figure 4.6 shows the particle size distributions after six pump passages at 750 rpm and 1800 rpm. The consequence of the increased pump speed now is very clear, with only 5% of nodules left in the original size class at 1800 rpm compared with 40% at 750 rpm. The increase in the  $63 < d < 0 \mu\text{m}$  size class even amounts to 20% at 1800 rpm. Abrasion in the hydrocyclone is expected to have greatly contributed to the production of fines since the sequential experiments took much more time than single passage experiments, thereby promoting the abrasion process.

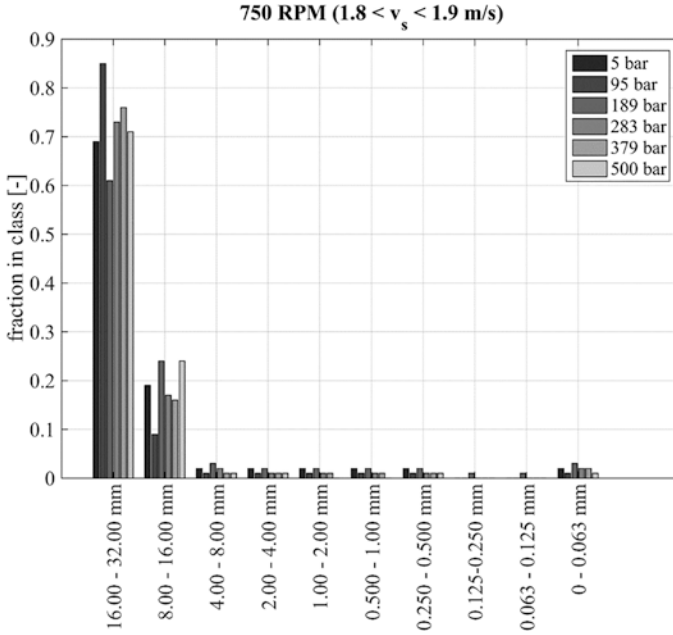
The impact fragmentation experiments in the pressure tank at NIOZ showed that for ambient pressures in the range of  $5 \leq p \leq 500$  bar, the ambient pressure has no significant influence on the nodule fragmentation. The experiments showed that nodule degradation in the pump.

strongly relates to the nodule velocity and the speed of the impeller, as expected due to the large energy of the impeller.

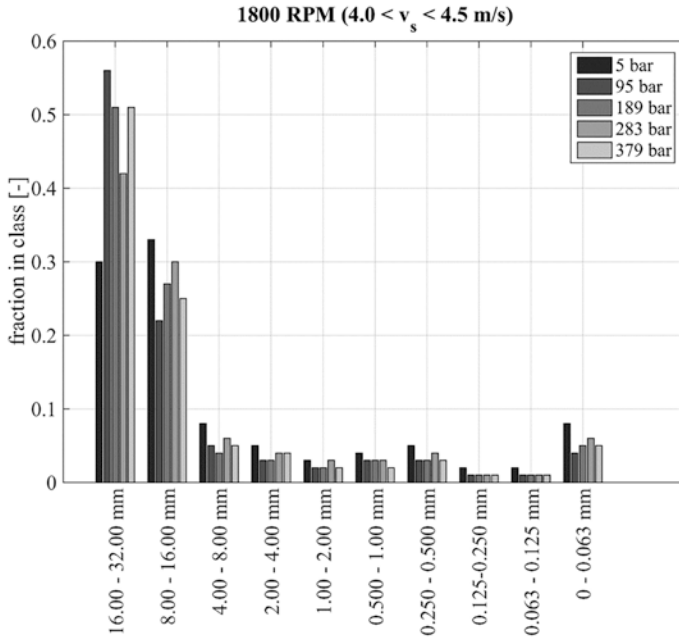
After the experiments at NIOZ with nodule fragments, there was a need to better understand the actual impact mechanics and degradation rates of intact nodules. Therefore, atmospheric impact experiments were conducted at well-controlled



**Fig. 4.4** Centrifugal pump test rig at NIOZ and typical nodule fragments. **(a)** Overview of the test setup. Nodule carousel (1), suction tube (2), pump (3) and hydroclone (4) with drive (5). **(b)** Two pairs of electromagnetic probes for measurement of the nodule velocity at the suction inlet. **(c)** Cross-section of pump casing (4) showing the passage of the largest nodule (2) through the inlet (1), driven by the impeller (3). **(d)** Nodule fragments after one of the experiments, showing large fragments (upper left) and fines (bottom left). (From: van Wijk et al. (2019), Copyright 2020 Elsevier, reprinted with permission)



a. 750 RPM test.



b. 1800 RPM test.

**Fig. 4.5** Comparison of PSD at different ambient pressures at two different pump speeds and associated fluid velocities in the suction pipe. The ambient pressure hardly has an influence on nodule degradation, while pump speed does have an influence. (a) 750 RPM test. (b) 1800 RPM test. (From: van Wijk et al. (2019), Copyright 2020 Elsevier, reprinted with permission)

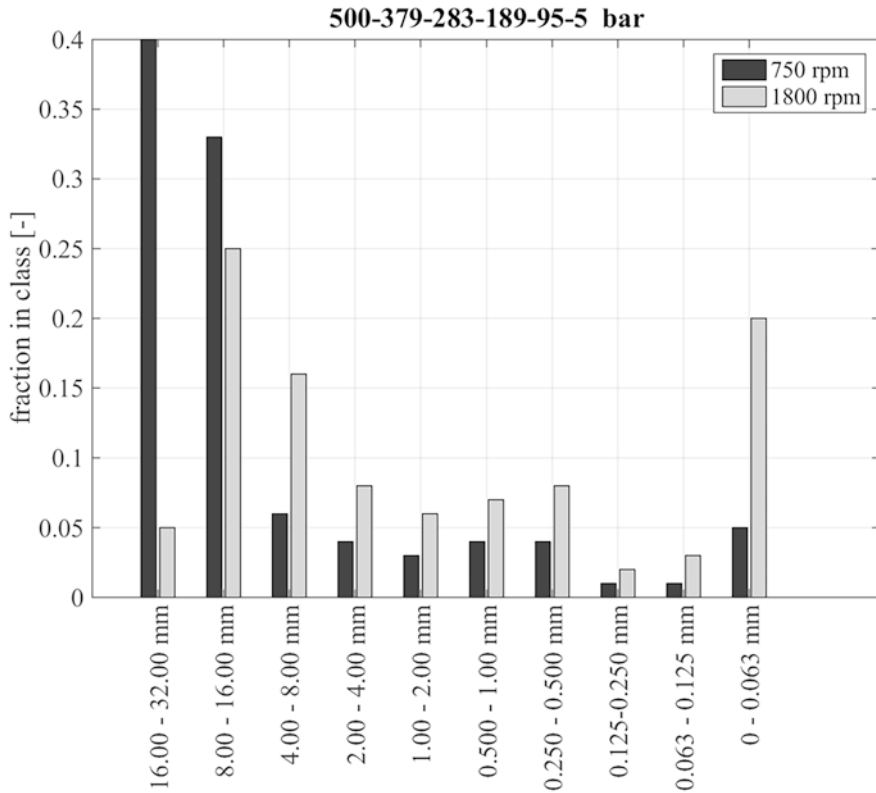


**Fig. 4.6** Particle size distributions of two experiments at two velocities, in which a sequence of pump passages was simulated that a nodule would experience upon transport through the VTS with a decreasing ambient pressure from 500 to 5 bar. Note the stronger effect of degradation due to increased pump revolutions. Also note the vast increase in fines (0–0.063 mm), which is caused by a large increase in abrasive wear in the hydrocyclone. (From: van Wijk et al. (2019), Copyright 2020 Elsevier, reprinted with permission)

impact velocities  $v = 4, 6$  and  $8$  m/s (van Wijk et al., 2019; van Wijk & de Hoog, 2020). The experiment consisted of a perpendicular impact of a nodule with a steel plate, on top of which a thin layer of water was applied, as shown in Fig. 4.7. This water has the function to mimic the presence of water during submerged impact, where the water acts as a buffer that dampens the impact.

The nodule diameters were in the range  $16 < d < 90$  mm and prior to testing the compressive strength was measured with a UCS test setup, which was correlated to tensile strength. A decreasing tensile strength was measured with increasing particle size, with more than a factor of ten difference in tensile strength between the largest and smallest nodules.

The particle size distributions of the nodules after the impact and the peak-stress at impact as a function of nodule diameter and impact velocity were measured. Particle size distributions are shown in Fig. 4.8. Chipping (i.e. small debris, but the

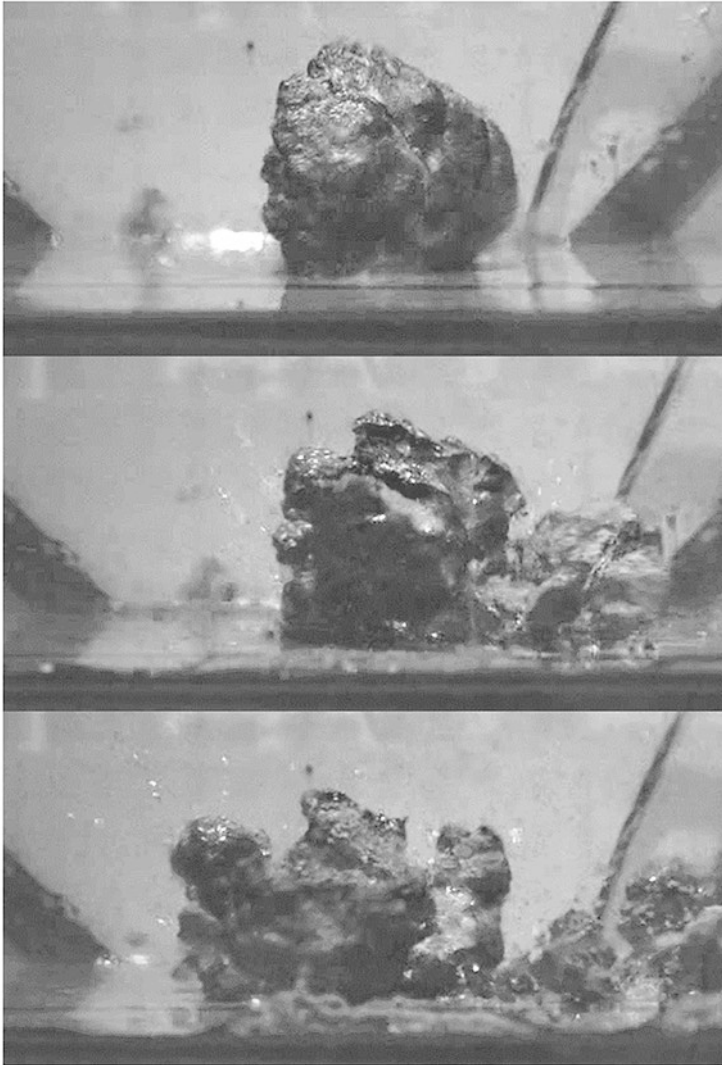
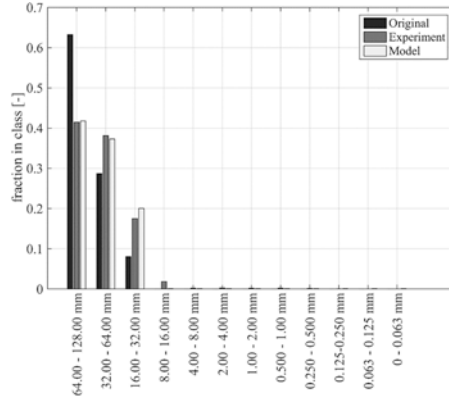


**Fig. 4.7** Video stills of a polymetallic nodule colliding with a wet steel plate. The nodule breaks into a few large pieces, and there is a limited amount of debris. (From: van Wijk et al. (2019), Copyright 2020 Elsevier, reprinted with permission)

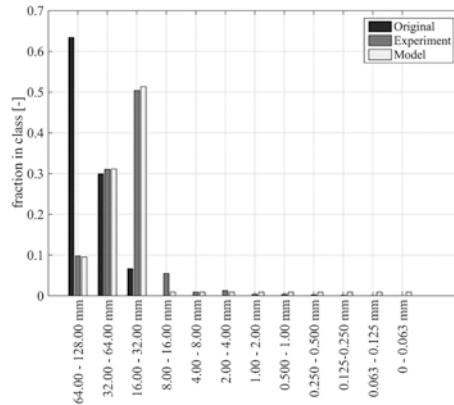
main nodule remains intact) was observed in the size range  $30 < d_m < 60$  mm and full fragmentation for the size class  $d_m > 60$  mm. Below  $d_m = 30$  mm no significant damage was observed. The results suggest a lower limit in particle size for the nodules being susceptible to impact fragmentation under the investigated conditions.

With the atmospheric experiments, it was possible to demonstrate that the production of fine material due to pure fragmentation is substantially smaller than

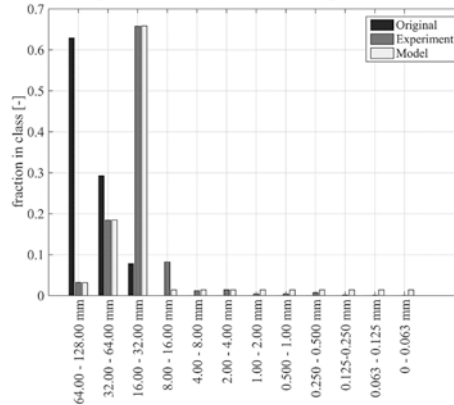
**Fig. 4.8** Original, and measured and predicted PSD after single impact. (a) Nodule fragment sizes after single impact with  $v = 4$  m/s. (b) Nodule fragment sizes after single impact with  $v = 6$  m/s. (c) Nodule fragment sizes after single impact with  $v = 8$  m/s. (From: van Wijk and De Hoog, (2020), Copyright Elsevier 2020, reprinted with permission)



a. Nodule fragment sizes after single impact with  $v = 4$  m/s.



a. Nodule fragment sizes after single impact with  $v = 6$  m/s.



a. Nodule fragment sizes after single impact with  $v = 8$  m/s.

found at NIOZ. The atmospheric experiments resulted in more rapid degradation of the nodules compared to the NIOZ experiments, which is thought to be related to the use of intact nodules instead of fragments, an argument supported by the relation between strength and nodule size.

### 2.3 Abrasion and Chipping in the Jumper and Riser Segments

While impact fragmentation is the dominant degradation mechanism in pumps, abrasion and chipping are the main causes of degradation in the jumper hose and riser system. To quantify these effects, dedicated abrasion and attrition experiments are needed (de Hoog et al., 2020).

The jumper, which is associated with a sliding bed with shear layer and thus abrasion and attrition of the nodules, leads the slurry into the VTS. In the riser, two mechanisms dominate the degradation process: (i) abrasion by sliding along the riser segments, which will mainly affect nodules close to the wall, and (ii) particle–particle interaction.

Different particle fractions with different sizes have different transport velocities and their relative velocities give rise to collisions and probably mild impact fragmentation, chipping and attrition. Particle–wall interaction will have velocities in the order of the mixture bulk velocity (several meters per second) in the axial direction, resulting in sliding contact. Radial particle velocities will be very limited. Particle–particle interaction will have velocities in the order of the hindered settling velocity. Typical hindered settling velocities range between 0 and 1 m/s for polymetallic nodules of tens of millimetres size, which is an order of magnitude smaller than the bulk velocity.

Abrasion takes place due to interaction between the asperities on the sliding surfaces and the effective contact area. In the contact area, abrasion is dominated by plastic deformation as a result of the normal load on the surfaces. This process is independent of the relative velocity of the moving bodies but fully dependent on the normal force and sliding distance.

The relation between particle degradation and horizontal hydraulic transport has been studied for the transport of coal. Worster & Denny (1955) made an important contribution by relating the degradation of coal to the velocity and transport distance of the coal in mainly stratified flow regimes with a sliding bed with saltation of coal lumps on top of it. Degradation relates to the combined effect of abrasive wear in the bed layer and attrition in the shear layer (particle–particle interaction). They report a strong relation between degradation and mixture velocity ( $\sim v_m^3$ ) and a weaker relation with sliding distance ( $\sqrt{s}$ ), pointing at a dominant chipping process even in sliding bed flow with saltating particles.

De Hoog et al. (2020) were able to quantify the specific wear rates (in conjunction with Archard's abrasive wear theory) of nodules sliding on PVC by using a continuously tilting test tube setup, as shown in Fig. 4.9, which is deemed a good proxy of jumpers and riser systems with liners. When calculating sliding distances and contact forces between nodules and the pipeline, Archard's theory then allows



**Fig. 4.9** Front view of the tilting pipe setup. A transparent PVC pipe, an electric motor and a crankshaft system to ensure a continuous tilting motion. (From: de Hoog et al., 2020. Copyright Elsevier 2020, reprinted with permission)

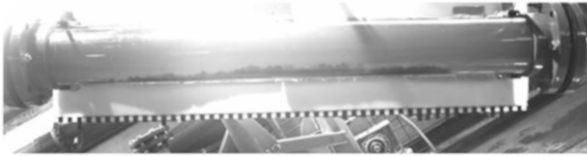


**Fig. 4.10** Sliding of the batch of nodules inside the experimental setup. High-speed videos were used to track the position of the particles. (From: de Hoog et al., 2020. Copyright Elsevier2020, reprinted with permission)

for calculating the overall production of fines due to abrasion. The tilting pipe batch experiment degradation process includes, on top of particle-wall abrasion, particle-particle abrasion and attrition as particles saltate and roll over each other, as shown in Fig. 4.10. This increases the number of collisions, as nodules are practically in constant contact with each other, with a higher degradation rate as a result. However, production of the finest fractions, as shown in Fig. 4.11, is attributed to abrasion only. A more detailed view on the abrasion of a single nodule is given in Fig. 4.12, which shows the ratio of mass loss due to abrasion over the normal force and the particle density, plotted as a function of sliding distance.

The tilting pipe batch experiments showed that degradation causes accumulation of material in the size of  $0.1 < d < 2.0$  mm, as apparent in Fig. 4.13. These classes tend not to degrade further, as they become suspended by the fluid, or trapped between the pores of the sliding nodule bed. As such, if hypothetically degradation would continue to a point where the sliding bed is fully degraded into suspended



**Fig. 4.11** The nodule batch after the experiments (left), the developed fines due to degradation (right). (From: de Hoog et al., 2020. Copyright Elsevier 2020, reprinted with permission)

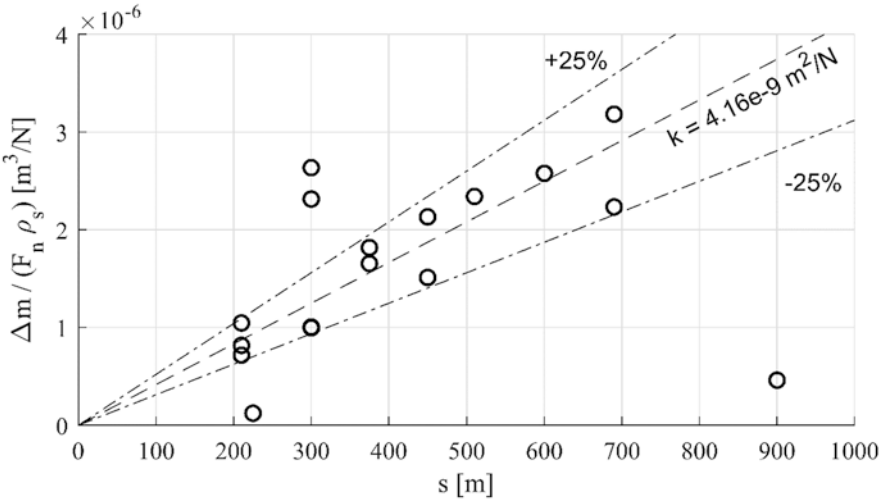


**Fig. 4.12** Ratio of mass loss over the normal force and the particle density, plotted as a function of sliding distance. This mass loss is caused by pure abrasive wear, tested on a single nodule in the tilting pipe setup. (From: de Hoog et al., 2020. Copyright Elsevier 2020, reprinted with permission)

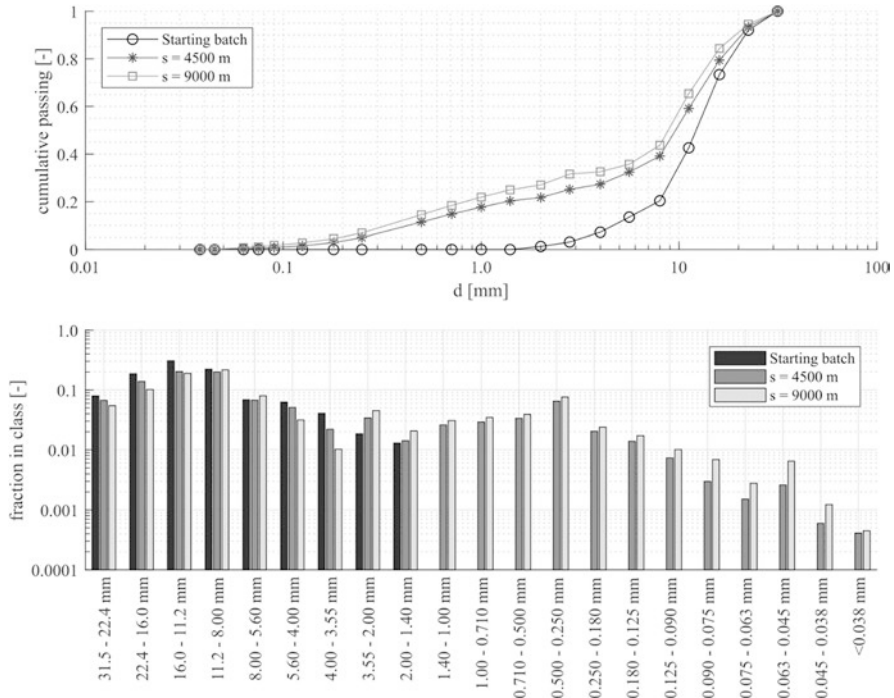


**Fig. 4.13** The initial batch PSD and the remaining PSD after a sliding distance of 4500 m and 9000 m, displayed in PSD (top) and bar plot (bottom). (From: de Hoog et al., 2020. Copyright Elsevier 2020, reprinted with permission)

particles, it would be expected to have the final PSD to be similar to the distribution of the  $0.1 < d < 2.0$  mm classes depicted in Fig. 4.13. Only a small portion of this is smaller than  $63 \mu\text{m}$ , considered economically unattractive to recover.

Vertical fluidization experiments were then conducted to mimic interactions between nodules as they would occur in the VTS under representative conditions, since the relative velocities are governing the chipping process rather than the mixture bulk velocities. In these experiments, a bed of nodules was fluidized and kept at a more or less stable position in the fluidization column at a volumetric concentration comparable to those occurring in the VTS. In this way, it was possible to avoid the degradation of nodules due to the centrifugal pump, while maintaining representative relative particle velocities. The test setup is depicted in Fig. 4.14.

Results show combined abrasion and attrition through particle-wall and particle-particle collisions. The amount of collisions was less frequent than in the tilting pipe saltating degradation process. This was due to the nature of the fluidization experiment, where particles are spaced farther apart than in a saltating flow. The overall degradation was significantly higher in the vertical flow experiment than in the sliding experiment, suggesting that degradation in the vertical flow experiment is dominated by attrition and chipping due to particle-wall and particle-particle collisions,

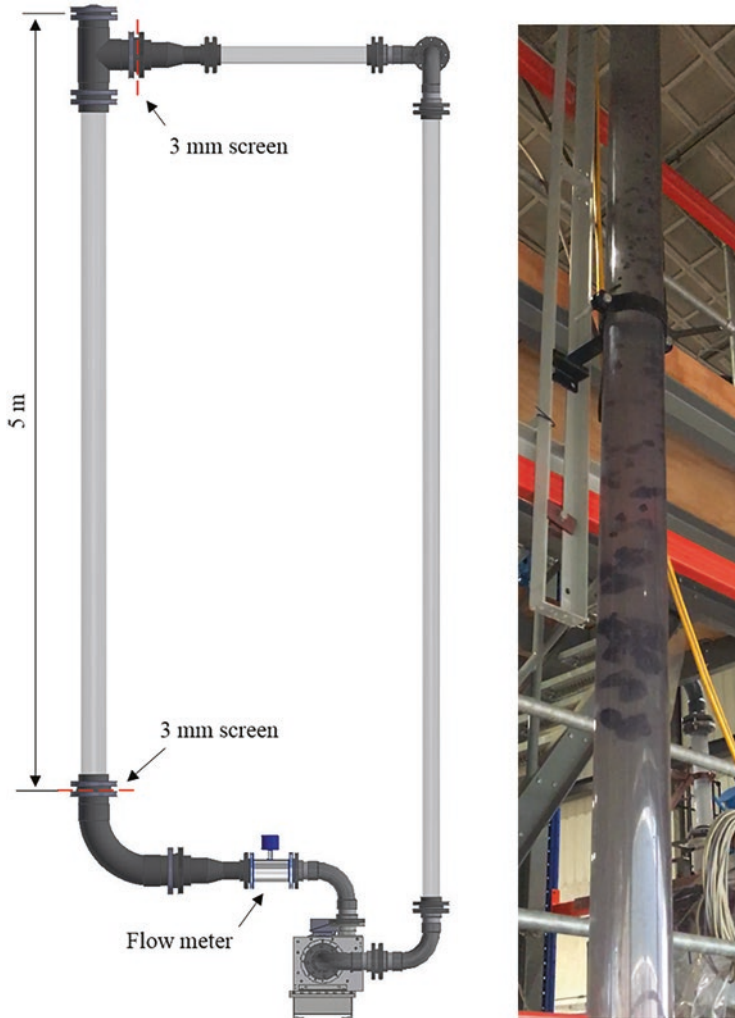


**Fig. 4.14** The vertical fluidization flow loop. (From: de Hoog et al., 2020. Copyright Elsevier 2020, reprinted with permission)

and there is very little abrasion. Figure 4.15 gives a general picture of the nodule fragments and grit produced during these experiments. Similar to the tilting pipe batch experiments, degraded particles tend to accumulate in the  $0.1 < d < 2.0$  mm size classes (see Fig. 4.16), because these sizes become suspended in the fluid and practically do not contribute to the degradation process.



**Fig. 4.15** Fragmented nodules and fines. (From: de Hoog et al., 2020. Copyright Elsevier 2020, reprinted with permission)

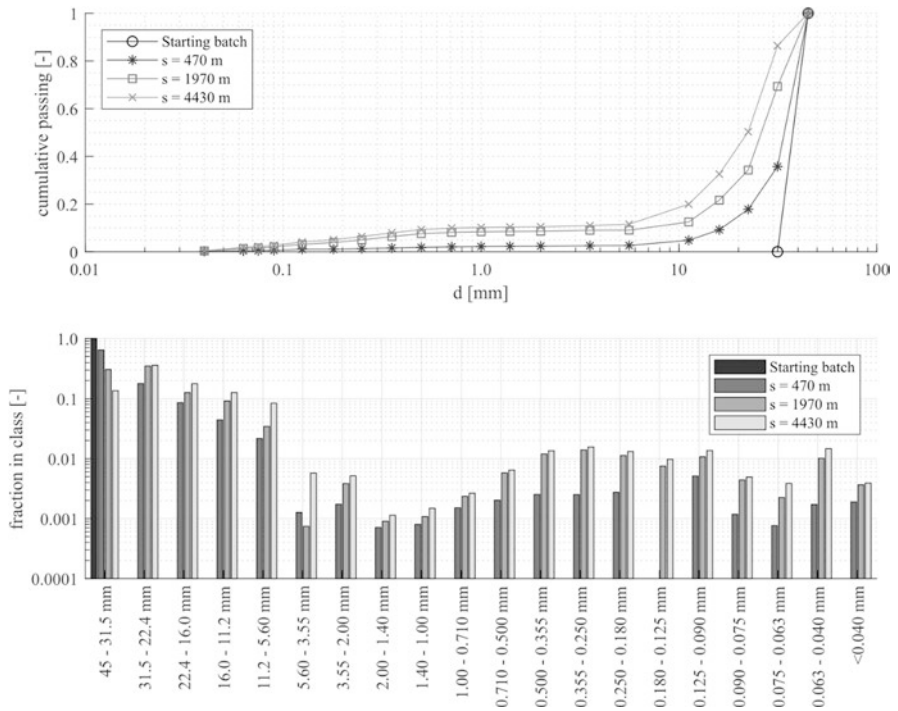


**Fig. 4.16** Change of particle size in the vertical fluidization experiment starting with nodules of the 45–31.5 mm class and three consecutive experiments, displayed in PSD (top) and bar plot (bottom). (From: de Hoog et al., 2020. Copyright Elsevier 2020, reprinted with permission)

**Table 4.2** Overview of hydraulic transport degradation mechanisms and their effect on the initial nodule PSD

| VTS component | Degradation mechanism | Effect on PSD                                                                                                          |
|---------------|-----------------------|------------------------------------------------------------------------------------------------------------------------|
| Pumps/bends   | Impact fragmentation  | Strong reduction of $d_{50}$                                                                                           |
| Jumper        | Abrasion/attrition    | Creates mainly new fractions $0.1 < d < 2.0$ mm. Small amount of fines $d < 63$ $\mu\text{m}$                          |
| Riser         | Abrasion/attrition    | Moderate decrease of $d_{50}$ . Creates new fractions $0.1 < d < 2.0$ mm. Small amount of fines $d < 63$ $\mu\text{m}$ |

## 2.4 An Integral Assessment of Nodule Degradation during Hydraulic Transport

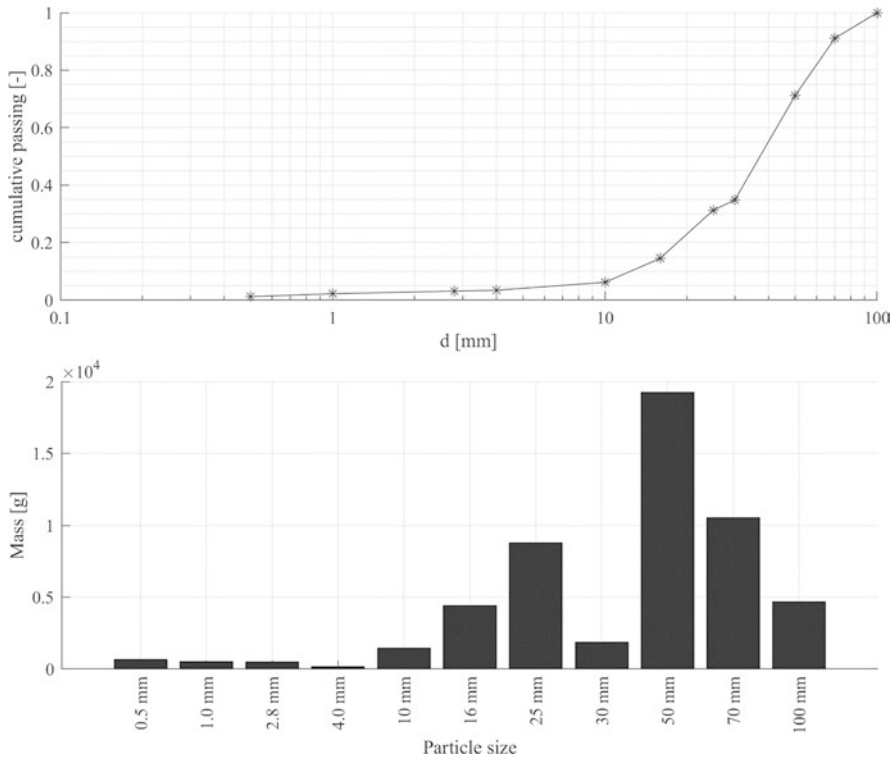
Having quantified the response of CCZ nodules to impact fragmentation, abrasion and chipping under conditions comparable to those during operation, it is possible to make an integral assessment of the development of the PSD during transit. Regarding impact fragmentation, a mathematical framework of a predictive model was provided in Van Wijk and de Hoog (2020), to aid in the design of a deep-sea mining operation.

Table 4.2 summarizes the degradation mechanisms encountered during vertical transport and their relative effect on the PSD of the nodules. The relative contribution of each mechanism depends on the configuration of the transport system. Knowledge of the different flow regimes in the various segments of the transport system, the associated degradation process and dedicated calculation models for the flow process, fragmentation, abrasion and chipping are required to make this integral assessment.

These results are based on tests conducted with CCZ nodules from the Belgian License area. Nodules with different mechanical properties will have different strengths and will result in different degrees of degradation. The framework provided in Van Wijk and de Hoog (2020) will allow for the quantification of degradation rates when actual nodule samples from the envisaged license area are available. Fortunately, if the size and density are somewhat comparable, the trends in Table 4.2 will be similar since this mainly depends on flow-related mechanisms.

## 3 Mechanical Response of Dry Bulk Material

The nodules that remained from the tests described in the previous sections have been utilized to study the mechanical response of the nodules as a bulk material. As generally known, the response of the bulk behaviour highly depends on particle shape and size distribution. Therefore, it is strongly advised to conduct comparable tests and analyses resembling realistic mining conditions. The particle properties of



**Fig. 4.17** PSD of nodules used for dry bulk behaviour. (Doorn, 2022. Reprinted with permission)

the nodules arriving at the vessel might differ significantly based on nodule characteristics at the bed, collection method and means of vertical transport, as discussed in Sect. 2. Here, an overview of the type of tests that were conducted to study the behaviour of the nodules in dry conditions is presented (Doorn, 2022).

Based on the nodule materials remaining after the fragmentation tests described in sect. 2, approximately 50 kg of nodules were available. Nodules were sorted for size based on sieving, the larger nodules were sorted by hand to avoid fragmentation. The resulting PSD is shown in Fig. 4.17. The exact history of these nodules is not known. The quality of storage conditions is questionable, especially regarding whether the nodules were stored wet. In our experiments, the nodules were again stored in water to saturate them. Then the saturated density of the nodules was measured as  $1911 \pm 35 \text{ kg/m}^3$ . After oven drying for 24 h at  $105 \text{ }^\circ\text{C}$ , the dry density was  $1341 \pm 46 \text{ kg/m}^3$ .

The angle of repose represents the shear stress of bulk material under the force of gravity. The angle of repose results are helpful to categorize the flow granular flow properties. In this research, the angle of repose is measured following the ledge test procedure, often referred to as ‘shear box’ and ‘rectangular container test’ (cf. Fig. 4.18). During a ledge test, a container was filled with granular material, after



**Fig. 4.18** Shear box test setup (Doorn, 2022). Reprinted with permission

which one side of the container was opened for the material to slide and roll out until an equilibrium was reached. The angle of repose was the resulting angle between the horizontal plane and the free surface. Due to the quantity of nodules and the size of the container, only the batch of nodules at a size of 10–16 mm was thoroughly tested. The angle of repose, based on 18 tests, is  $49.5^\circ \pm 1.46^\circ$  and  $49.6^\circ \pm 1.1^\circ$ , respectively, for saturated and dry nodules. Dreiseitl (2017) measured substantially lower angles of repose of  $30^\circ$  and  $33^\circ$  for intact nodules recovered from box-cores (Fig. 4.18).

An inclined surface tester (cf. Fig 4.20) was used to measure the sliding and rolling friction of particles along various materials commonly employed in bulk handling equipment, such as steel (S235) and rubber (Ethylene Propylene Diene Monomer). The tester employs a motor to adjust the inclination of the bottom surface, where the steel or rubber plate is mounted. The angle between the inclined surface and the horizontal is referred to as the inclination angle. The sliding and rolling response of individual nodules depends significantly on how constrained their motion is due to neighbouring particles. Therefore, several tests were conducted as follows (cf. Figure 4.19):

1. Single nodule.
2. Free movement of batch of nodules.
3. Confined movement of batch of nodules.
4. Added mass rolling configuration.
5. Added mass sliding configuration. Nodules are confined in a mould, restricting the nodules from rolling and forcing them to slide.

### 3.1 *Single Nodule*

In the ‘single nodule’ test, it was observed that when using rubber as the bottom surface, the primary mode of movement was rolling. On the other hand, when employing a steel plate, the primary mode of movement was sliding. No significant

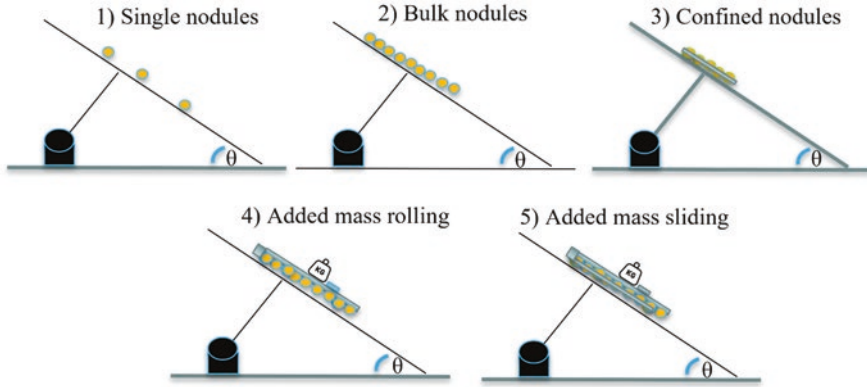


**Fig. 4.19** Conducted sliding and rolling friction for single and bulk nodules. (Doorn, 2022. Reprinted with permission)

**Table 4.3** Recorded angle at which the nodule starts to move

| <b>Rubber</b> |                   | <b>Dry</b>          | <b>Saturated</b> |
|---------------|-------------------|---------------------|------------------|
| Count [-]     |                   | 18                  | 16               |
| Mean [°]      |                   | 30.4                | 29.2             |
| Std           |                   | 2.7                 | 2.7              |
| <b>Steel</b>  | <b>Dry smooth</b> | <b>Dry corroded</b> | <b>Saturated</b> |
| Count [-]     | 39                | 23                  | 16               |
| Mean [°]      | 19.8              | 28.4                | 27.7             |
| STD [°]       | 0.8               | 1.5                 | 1.7              |

Doorn (2022). Reprinted with permission

difference was observed between dry and saturated nodules. However, it was noted that the response of a single nodule on the steel plate was affected by whether the plate was corroded or not. As a result, tests were conducted with freshly polished steel plates and with corroded plates resulting from the experiments with the fresh plates. The surface roughness of the plates was measured with a profilometer, indicating roughness values of  $0.46 \pm 0.07$  and  $1.16 \pm 0.12 \mu\text{m}$  for the smooth and corroded plates, respectively (see Table 4.3) (Figs. 4.20 and 4.21).

### 3.2 Layer of Nodules

Similar tests were conducted for a single layer of particles. Here, it was tested as to at what angle the majority of the particles started to slide or roll. This typically occurs with many of them moving altogether, behaving mostly like a granular flow. Additional tests were conducted, with the particles being constrained to remain together by means of a water-resistant paper wrapped around the batch of nodules. Results from both sets are shown in Table 4.4.

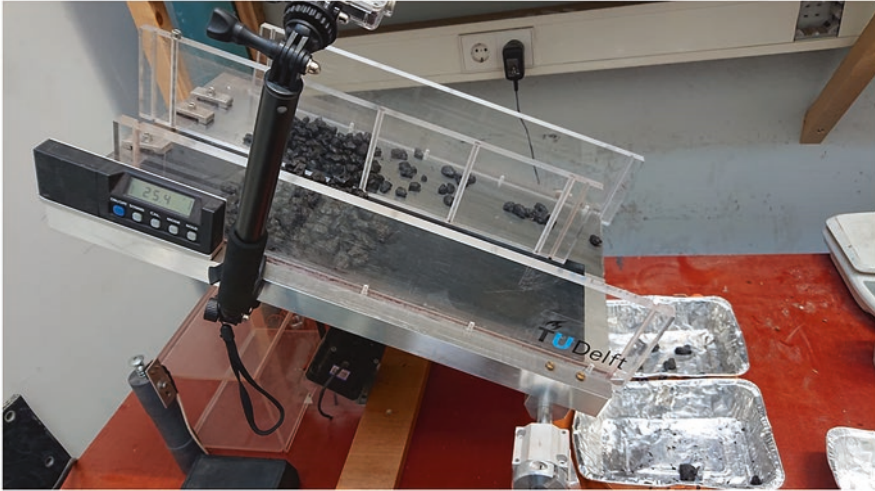


**Fig. 4.20** Tilting table at the initiation of sliding/rolling of a set of nodules. (Doorn, 2022. Reprinted with permission)

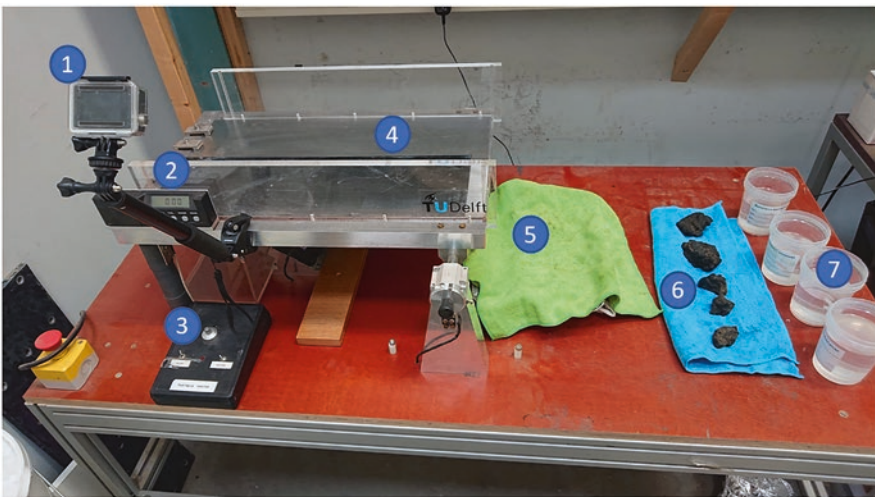


**Fig. 4.21** Tilting table setup. (Doorn, 2022. Reprinted with permission)

### 3.3 *Layer of Nodules under Normal Load*

Finally, a set of experiments was conducted where a normal force was applied on top of the particles, simulating a layer of particles above. As depicted in Fig. 4.19, one set of tests comprised a sledge mounted on top of the nodules with an additional mass, increasing the applied normal force on the nodules. The other set of tests utilized a matrix of nodules embedded in plaster, effectively interlocking the layer

**Table 4.4** Inclination angle at which bulk starts to slide/roll Doorn (2022). Reprinted with permission

| <b>Rubber</b>  | <b>Dry</b>            | <b>Dry (constrained)</b>                | <b>Saturated</b> | <b>Saturated (constrained)</b> |
|----------------|-----------------------|-----------------------------------------|------------------|--------------------------------|
| Count          | 8                     | 13                                      | 8                | 14                             |
| Mean [°]       | 30.1                  | 32.9                                    | 30.2             | 31.6                           |
| 95% confidence | 2.7                   | 1.1                                     | 1.6              | 1.0                            |
| <b>Steel</b>   | <b>Dry (corroded)</b> | <b>Dry (constrained &amp; corroded)</b> | <b>Saturated</b> | <b>Saturated (constrained)</b> |
| Count          | 8                     | 17                                      | 8                | 14                             |
| Mean [°]       | 26.2                  | 30.6                                    | 30.2             | 33.7                           |
| 95% confidence | 1.0                   | 0.8                                     | 2.1              | 1.3                            |

**Table 4.5** Friction angle found under added normal force. Doorn (2022). Reprinted with permission

| <b>Rubber</b> | <b>Dry</b> | <b>Saturated</b> |
|---------------|------------|------------------|
| Count         | 18         | 18               |
| Mean [°]      | 32.48      | 30.54            |
| STD [°]       | 4.88       | 3.25             |
| <b>Steel</b>  | <b>Dry</b> | <b>Saturated</b> |
| Count         | 18         | 18               |
| Mean [°]      | 28.28      | 30.07            |
| STD [°]       | 3.27       | 3.76             |

of nodules on the bottom surface. The mass added on top of both the nodules cast and the sledge was 3 kg, equivalent to a mass of approximately 330 kg/m<sup>2</sup>. Once again, tests were carried out for both dry and saturated nodules, and the results are presented in Table 4.5.

### 3.4 Findings

It has been observed that the behaviour of saturated nodules differs slightly from that of dry nodules. When nodules are in contact with steel equipment (e.g. hopper), dry nodules tend to exhibit a lower friction angle of approximately 2°. Conversely, when in contact with rubber (e.g., conveyor belt), dry nodules tend to have a higher friction angle compared to saturated nodules. Furthermore, during sliding along the steel plate, nodules experience sliding wear, which was not observed in the case of rubber. The exact reasons for these differences in material response are not yet fully understood and could be related to (1) the particle density of the nodules and (2) the hardness of the contact surface and, consequently, the effective contact area. Further research into the micro-level phenomena at the contact interface between the nodules and equipment surface may provide insights into the underlying mechanisms.

## 4 Approaches to Breakage and Fines Generation in Biomass Handling

Deep-sea mining is not the only industry facing challenges related to the handling of fragile materials and issues concerning particle breakage, degradation and fines generation. These challenges are also prevalent in the biomass handling sector, although in a drier environment, with degradation mechanisms similar to those outlined in Table 4.1. An analogous handling chain to PmN can be found in biomass pellets, where it is crucial to prevent the undesirable generation of fines during handling. Additionally, the internal structure of the particles is inhomogeneous, and different degradation mechanisms occur depending on the handling method.

This section focuses on the experimental and numerical methods used in researching the handling of granular material and in particular biomass pellets, and how they can offer valuable insights for analyzing and designing handling solutions in the deep-sea mining industry.

### 4.1 Biomass Pellets

Though the formation processes of PmNs and man-made biomass pellets differ significantly, both internal structures exhibit inhomogeneities that act as weak spots susceptible to breakage.

Duliu et al. (1997) and Rizescu et al. (2001) utilized computer tomography to reconstruct PmNs (see Fig. 4.22a), revealing the inhomogeneity within the nodules' internal structure. They observed variations in nucleus shape and origin, primary and secondary growth surfaces, highly mineralized areas, and the presence of a fracture network.

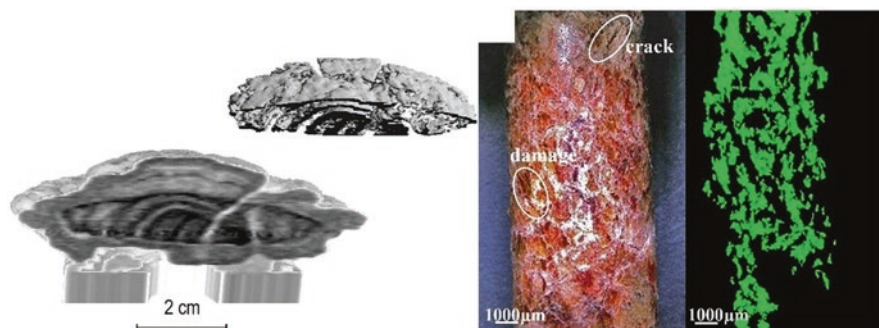


**Fig. 4.22** Left Image of PmN structure (From: Rizescu et al. (2001) Copyright Elsevier 2001, reprinted with permission) and right, Digital images and corresponding determined damage area of wood pellet. (From: Cutz et al. (2021). Copyright 2021 Springer Nature, reprinted with permission)

The process of creating biomass pellets involves grinding and passing dried biomass through a pellet die at high temperature and pressure. This results in the melting of lignin within the biomass, binding the particles together. After cooling, the particles reform into solid cylindrical-shaped pellets with uneven ends. As an example, Cutz et al. (2021) also employed CT to analyze the internal structure, uncovering fractures both on the surface and inside the particles (see Fig. 4.22b).

## 4.2 Experiments to Assess Breakage

Experimental techniques to determine the tendency of particles to break and evaluate their breakage characteristics include:

- Compression testing: Involves subjecting particles or specimens to compressive forces by uniaxial or triaxial tests to evaluate their resistance to breakage and analyzing the resulting particle size distribution.
- Impact testing: Evaluates the susceptibility of particles to breakage under impact or collision forces by analyzing the generated fragments and assessing fragmentation patterns (Sect. 2.2).
- Shear testing: Particularly useful for cohesive particles or materials with inter-particle bonding, where particles are subjected to shear forces to simulate sliding or movement. Changes in particle arrangement and breakage are analyzed.
- Tumbling tests: Simulates continuous or repetitive tumbling and rolling motion to assess particle breakage, measuring changes in particle size distribution or fines generation (Sect. 2.3).
- Attrition testing: Evaluates particle tendency to undergo attrition or abrasion by subjecting particles to abrasive conditions and quantifying particle wear, loss of material and changes in size or shape.
- Particle size distribution analysis: Indirectly assesses particle breakage by comparing particle size distribution before and after a treatment or testing, using techniques like sieve analysis, laser diffraction or image analysis.

The choice of test should be relevant to the actual conditions of the handling process. In the case of biomass wood pellets, Gilvari et al. (2019) analyzed reported tests in the literature and concluded that the enormous variety of often tailor-made tests inspired by other domains makes it difficult to compare results due to the absence of a prescribed overall standard.

Encouraging the development of standards is important to have unified tests adopted by all parties in the handling chains. Furthermore, using standards and obtained experimental data under representative operational conditions allows for necessary validation data for modelling of breakage in the supply chain.

### 4.3 Biomass Handling Experiments

To gain insights into the various handling stages of the biomass handling chain, a comprehensive analysis was conducted (Gilvari, 2021). This analysis involved multiple testing methods, including compression testing of individual particles (Gilvari et al., 2021a, b), tumbling tests (Gilvari et al., 2020), impact testing and laboratory-scale bulk handling tests under different operational conditions (cf. Fig. 4.23) (Gilvari et al., 2022) and industrial-scale testing and analyses of fines generation using particle size distribution analysis (Gilvari et al., 2021a, b). These testing approaches were systematically examined and integrated to provide a comprehensive understanding of the biomass handling chain at different scales (Gilvari, 2021).

The industrial-scale tests to evaluate the generation of fines and dust during handling processes were conducted on an existing handling chain at a port. Pellets were discharged from a seagoing vessel through a hopper onto a conveyor system, which transported the material to a silo. In addition to the continuous sampling system

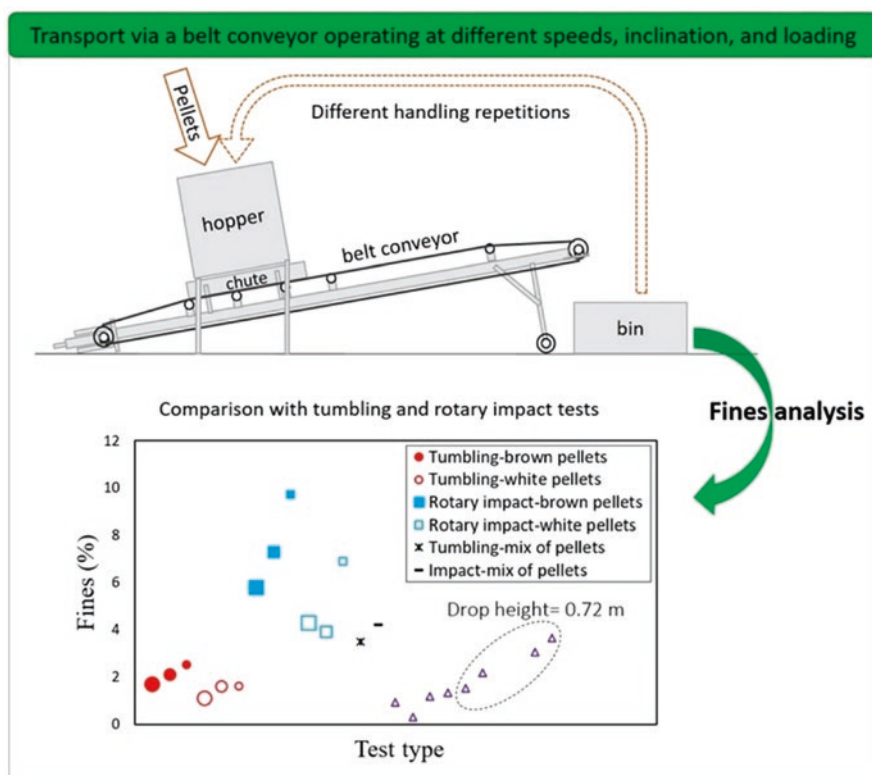


**Fig. 4.23** Schematic of the laboratory setup and results of analysis of the effect of repetitions on biomass pellet fines generation under operational conditions. (From Gilvari et al. (2022). Copyright, 2022, Elsevier, reprinted with permission)

installed for quality control, samples were collected at multiple points in the chain. The primary finding was that at a transfer point between two conveyors, the proportion of small particles (<5.6 mm) increased from around 9% to 14%. This highlights the significance of equipment design and operation in relation to material degradation.

These particle-level investigations also served as a basis for developing numerical models using the discrete element modelling approach, laying the groundwork for further studies on pellet breakage in handling systems.

#### 4.4 *Modelling Approaches*

The modelling of individual particle breakage can be accomplished using various methods. For example, finite element modelling allows the material to be described as a continuum and can incorporate fracture criteria to simulate particle breakage under different loading conditions. However, due to the granular nature of the material and the necessity to model the entire system (equipment and granular material interactions), discrete element modelling (DEM) is a more suitable approach. DEM, first proposed by Cundall and Strack (1979), represents individual particles as discrete elements and considers their interactions based on contact mechanics principles. DEM models can include parameters like particle strength, fracture toughness, and critical stress for breakage simulation. Moreover, DEM naturally allows fragmented parts to continue as smaller particles.

By tracking particle movements and forces, DEM can offer insights into individual particle breakage patterns, overall bulk material behaviour and the performance of the entire system, including forces, power, wear, and material flow. After defining input parameters and calibrating and validating with experimental data under representative operational conditions, DEM becomes a powerful tool for designing material handling equipment. For example, Schott et al. (2021) introduced a design framework successfully used for novel granular material handling equipment, along with full-scale validation. To develop such models describing particle-particle and equipment interactions, defining input parameters is crucial. This requires experimental data at the interface between material and equipment, as discussed in Sects. 2 and 3.

Figure 4.24 (Jiménez-Herrera et al., 2018) illustrates three ways of modelling particle breakage in DEM simulations. The bonded-particle model (BPM) shows bonds that can break when stressed beyond a critical level. The fast-breakage model (FBM) employs polyhedral elements and is a particle-replacement model, potentially powerful for simulating large-scale comminution systems, provided that the models describing the breakage probability and distribution offer the necessary degrees of freedom. In the particle replacement model (PRM), the simulation removes the spherical parent particle when the fracture occurs and replaces it with a set of progeny particles

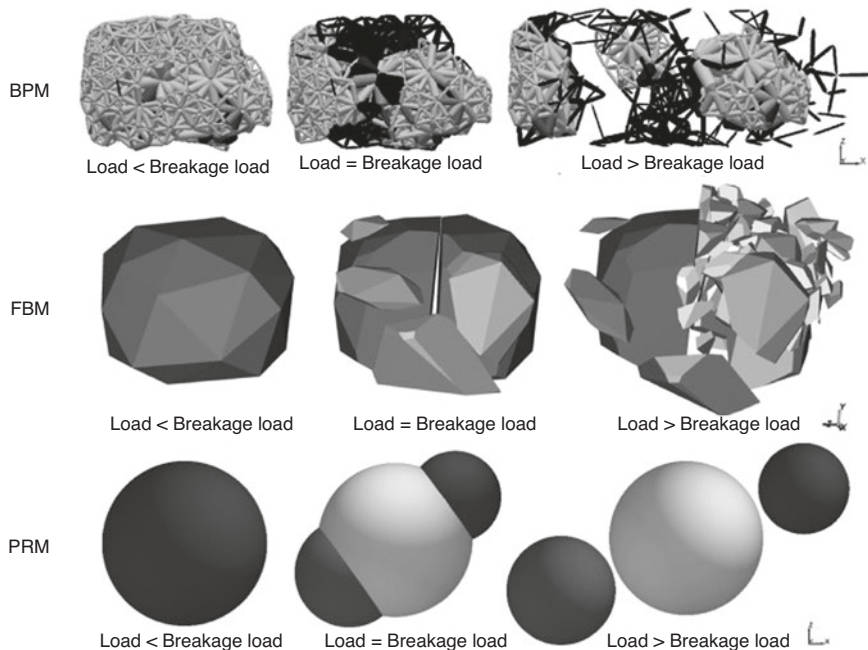


**Fig. 4.24** Simulation stills of breakage of single particles: In the BPM, the particle is represented by means of their bonds (light grey: unstressed; gray: stressed; black: broken). In the FBM, primary breakage occurs when the stressing energy surpasses the breakage energy and secondary afterwards. In the PRM, only primary breakage is illustrated, with an additional moment after that. Load applied in the vertical direction. (From: Jiménez-Herrera et al. (2018). Copyright Elsevier 2018, reprinted with permission)

In the comparison of these three models, Jiménez-Herrera et al. (2018) concluded that each model possesses unique strengths. The particle-replacement method (PRM) demonstrated an excellent fit for the size distribution of the progeny from both single-particle breakage and particle bed experiments, making it an appealing alternative to previous models, especially when simulating large particle populations.

Tavares (2022) presents a critical analysis of his comprehensive mathematical breakage model suitable for describing the breakage of populations of brittle materials in conjunction with the discrete element method, either as part of particle replacement schemes or coupled to it in microscale population balance models. This breakage model has been extensively used in advanced models of crushers and various mills, enabling the prediction of degradation during material handling, including iron ore pellets. To be effective in such models, it is crucial to understand the particle response under various conditions encountered in a system that can cause mechanical degradation. These conditions encompass diverse particle sizes, stressing intensities, geometries, rates of stressing and modes of stress application. Furthermore, he notes that challenges persist in estimating breakage parameters for

fine particles, despite models accounting for essential variables. Additionally, models describing surface breakage play a crucial role in predicting mechanical degradation during handling, demanding increased attention due to being in an early stage of development and validation.

#### **4.5 Biomass Pellets**

In the modelling of individual biomass pellets' breakage, Gilvari et al. (2021a, b) employed a bonded-particle model with the bonded contact based on the Timoshenko-Ehrenfest beam theory. Each pellet was represented by a varying number of 960–8000 spheres. Initially, uniaxial and diametrical compression tests were conducted on seven different types of biomass pellets in an experimental setup. The results revealed variations between pellets of different types and even within pellets of the same type due to heterogeneity in the pellet structure. This heterogeneity could be attributed to differences in the particle size distribution of the raw materials, heterogeneous porosity, presence of micro-cracks and other factors.

The maximum stress at failure for the tested pellets ranged from 8 to 32 MPa. The numerical outcomes demonstrated that the mechanical strength of various types of pellets could be represented by using the number of spheres and the coordination number as variables, in addition to the bond parameters. The calibrated model successfully predicted the stress-strain curves and modulus of elasticity of individual pellets and reasonably estimated their breakage behaviour under uniaxial and diametrical compressions.

However, it's worth noting that the amount and size of particles released from the pellets during compression tests were excluded both in the experimental and numerical aspects of the study. Building on Jimenez-Herrera et al.'s (2018) work and based on Gilvari's findings, it is recommended that fragmentation should be incorporated in the next stages of the modelling process. Moreover, considering the computational expenses associated with using the bonded-particle model, depending on the number of spheres used for a single particle, it may be unfeasible for modelling industrial scale systems.

#### **4.6 Next Modelling Steps**

To assess the performance of nodule handling equipment with respect to the breakage of nodules, generation of fines and consumption of energy, the DEM would be a suitable method to simulate the processes at the scale of the handling equipment. A set of standardized experiments to assess the relevant material characteristics of the nodules is necessary to allow for proper comparison of equipment and operations. Experiments like those presented in Sect. 2 provide a basis for such a standardized set. Such experiments should provide valuable information to allow for

calibration of the particle properties in DEM, which is necessary to mimic the breakage behaviour of PmN. To effectively model breakage behaviour in the context of deep-sea mining, with a specific focus on material behaviour and degradation, it is recommended to employ DEM in conjunction with a particle replacement method to accurately capture fragmentation. However, it is also important to take into account the development of models that describe surface breakage to further enhance the accuracy and comprehensiveness of the simulations. A promising approach is Tavares' mathematical breakage model suitable for describing the breakage of populations of brittle materials in conjunction with the discrete element method, again under the condition of availability of experimental data as elaborated in this chapter.

PmN is handled in a more complex environment, potentially requiring dedicated breakage models for submerged, moist and dry conditions. Similar aspects hold for the volumetric concentration of nodules in each of the handling steps, ranging from collision-dominated to contact-dominated material handling. Further research regarding the bulk behaviour of nodules, ranging from submerged to dry condition, is needed to allow for the generation of the standardized nodule granular and breakage properties. These, combined with calibrated models in DEM, will enable for optimization of the key handling steps and equipment.

## 5 Conclusions and Recommendations

For a sustainable (green, energy and cost-efficient) supply chain, it is important to carefully balance the processing capacity with the mining capacity and the expected demand for the final products to optimize the efficiency and effectiveness of the supply chain. This requires careful planning and coordination between all stakeholders involved in the deep-sea mining supply chain, including the mining and processing companies, logistics providers and end customers.

Hydraulic transport is one of the key technologies that is being considered for conveying the polymetallic nodules from the seafloor to the mining support vessel. Degradation of the polymetallic nodules is closely related to the hydraulic transport regime. Experiments have shown that, in the jumper hose predominantly abrasion and chipping occurred, in the riser attrition and abrasion, and in the centrifugal pumps predominantly impact fragmentation was observed.

These mechanisms have been studied in more detail with Polymetallic Nodules from the Belgian and UK CCZ license areas under various conditions. Research into impact fragmentation on polymetallic nodules fragments indicates that the pump impeller speed has a major influence on the degradation process, and no significant dependency on the ambient pressure (in the range of 5–500 bar) was found. These findings were confirmed in successive impact experiments, where nodules were subjected to perpendicular collision with a steel plate under atmospheric conditions at impact velocities up to 8 m/s. In general, impact was found to cause fragmentation of nodules down to mm scale without significant production of finer particles.

The tilting pipe batch experiments showed that degradation by sliding and particle collision causes accumulation of material in the size range of  $0.1 < d < 2.0$  mm, after which further degradation stops as debris becomes suspended in the fluid or settles within the pores of the sliding bed. A limited portion of the debris was found to be smaller than 63  $\mu\text{m}$ .

The degradation during the fluidization experiment was significantly larger than in the sliding bed experiment, suggesting that degradation in the vertical flow experiment is dominated by attrition and chipping due to particle–wall and particle–particle collisions. Nodule fragments and grit tend to accumulate in the  $0.1 < d < 2.0$  mm size classes, similar to the tilting pipe experiment, because these sizes become suspended in the fluid, and practically do not contribute to the degradation process. These results indicate only very little abrasion to take place during the actual vertical transport in the riser.

The mechanical response of nodules has been extensively studied through various tests and analyses. The behaviour of the bulk material is influenced by factors such as particle shape and size distribution, which vary based on nodule characteristics at the bed, collection method, and vertical transport means. The conducted experiments have provided valuable data on the angle of repose, sliding and rolling friction, and the effect of normal force on nodules. Understanding the differences between saturated and dry nodules in contact with different equipment surfaces calls for further research to uncover the underlying mechanisms at the micro-level interface.

A range of experimental techniques have been employed to determine particle breakage tendencies and evaluate breakage characteristics in various handling processes. These include compression testing, impact testing, shear testing, tumbling tests, attrition testing, and particle size distribution analysis. Encouraging the development of standardized tests is essential for reliable comparison of results and validation of breakage models from seafloor to mining support vessel. As an example from the context of biomass handling, comprehensive analyses integrating multiple testing methods at different scales have provided valuable insights into equipment design and material degradation, paving the way for further studies and numerical modelling of breakage in any handling system.

Various modelling approaches for particle breakage exist, with discrete element method being well-suited for granular materials and equipment interactions. DEM, along with particle replacement model, provides valuable insights into breakage patterns and bulk material behaviour, aiding in material handling equipment design. Challenges remain in estimating breakage parameters for fine particles and developing surface breakage models. The Tavares model is the state of the art describing the breakage of populations of brittle materials in conjunction with the discrete element method, either as part of particle replacement schemes or coupled with microscale population balance models. It is crucial to acknowledge that for particles to be effectively utilized in such models, their response must be understood across a range of conditions that they may encounter in real conditions. These conditions typically involve diverse particle sizes, stressing intensities, geometries, rates of stress and modes of stress application. To provide relevant input for these models,

standardized experiments to characterize nodules and bulk responses at these conditions should be developed. Once this is in place, the models can be used for optimizing handling steps and equipment in deep-sea mining.

**Acknowledgements** The authors would like to thank Floris Doorn for the extensive number of experiments he conducted during his master's in Offshore and Dredging Engineering at TU Delft, Paul Vercrujssse from DEME-GSR for providing us with nodules.

A very special thanks needs to go to Cees van Rhee, full professor in Dredging Engineering. As a pioneer, he was the first to introduce us to the exciting topic of deep-seabed mining. Cees unexpectedly passed away at the age of 64. We will remember him as a dear colleague and inspiring mentor.

## References

- Allseas. (2022). *Deep-sea polymetallic nodule collection*. Allseas.
- Beekman, W., Meesters, G., Scarlett, B., & Becker, T. (2002). Measurement of granule attrition and fatigue in a vibrating box. *Particle & Particle Systems Characterization*, 19(1), 5–11.
- Cundall, P., & Strack, O. D. L. (1979). A discrete numerical model for granular assemblies. *Géotechnique*, 29(1), 47–65.
- Cutz, L., et al. (2021). Microstructural degradation during the storage of biomass pellets. *Communications Materials*, 2(1).
- de Hoog, E. (2016). *Coarse particle slurry flow in inclined pipes and vertical S-bends*. MSc thesis TU Delft.
- de Hoog, E., In't Veld, J., van Wijk, J. & Talmon, A. (2017). *An experimental study into flow assurance of coarse inclined slurries*. Prague, Czech Republic, 18th international conference on the transport and sedimentation of solid particles.
- de Hoog, E., van Wijk, J., Wijnands, J., & Talmon, A. (2020). Degradation of polymetallic nodules during hydraulic transport under influence of particle-wall and particle-particle interaction. *Minerals Engineering*, 155, 106415.
- Doorn, F. (2022). *The effect of moisture on the granular characteristics of polymetallic nodules in the context of bulk handling*. TU Delft.
- Dreiseitl, I., 2017. *About geotechnical properties of the deep seabed polymetallic nodules*. Prague, Czech Republic, 18th international conference on the transport and sedimentation of solid particles.
- Duliu, O., Tufan, M., & Szobotka, S. (1997). Computer axial tomography investigation of polymetallic nodules. *Marine Geology*, 138(3–4), 303–311.
- Gilles, R., Haas, D., Husband, W. & Small, M. (1982). *A system to determine single pass particle degradation by pumps*. Johannesburg, South Africa, 8th international conference on the hydraulic transport of solids in pipes.
- Gilvari, H. (2021). *Degradation of biomass pellets during transport, handling and storage: An experimental and numerical study*. PhD thesis TU Delft.
- Gilvari, H., de Jong, W., & Schott, D. L. (2019). Quality parameters relevant for densification of bio-materials: Measuring methods and affecting factors – A review. *Biomass and Bioenergy*, 120, 117–134.
- Gilvari, H., De Jong, W., & Schott, D. L. (2020). The effect of biomass pellet length, test conditions and torrefaction on mechanical durability characteristics according to ISO standard 17831-1. *Energies*, 13(11).
- Gilvari, H., et al. (2021a). Large-scale transportation and storage of wood pellets: Investigation of the change in physical properties. *Particology*, 57, 146–156.

- Gilvari, H., de Jong, W., & Schott, D. L. (2021b). Breakage behavior of biomass pellets: An experimental and numerical study. *Computational Particle Mechanics*, 8(5), 1047–1060.
- Gilvari, H., et al. (2022). Fragmentation of fuel pellets during transport via a belt conveyor: A design of experiment study. *Particuology*, 66, 29–37.
- Jiménez-Herrera, N., Barrios, G. K., & Tavares, L. M. (2018). Comparison of breakage models in DEM in simulating impact on particle beds. *Advanced Powder Technology*, 29(3), 692–706.
- Laarhoven, B. V., Schaafsma, S., & Meesters, G. (2012). Toward a desktop attrition tester; validation with dilute phase pneumatic conveying. *Chemical Engineering Science*, 73, 321–328.
- Ma, W. (2019). *Sustainability of deep sea mining transport plans*. PhD thesis TU Delft.
- Ma, W., Van Rhee, C., & Schott, D. (2017). Technological and profitable analysis of airlifting in deep sea mining systems. *Minerals*, 7(8).
- Monhemius, A. (1980). The extractive metallurgy of deep-sea manganese nodules. In A. Burkin (Ed.), *Topics in non-ferrous extractive metallurgy – Critical reports on applied chemistry* (pp. 42–69). Blackwell Scientific Publication.
- Randhawa, N., Hait, J., & Jana, R. (2016). A brief overview on manganese nodules processing signifying the detail in the Indian context highlighting the international scenario. *Hydrometallurgy*, 165(Part 1), 166–181.
- Ravelet, F., Bakir, F., Khelladi, S., & Rey, R. (2013). Experimental study of hydraulic transport of large particles in horizontal pipes. *Experimental Thermal and Fluid Science*, 45, 187–197.
- Rizescu, C. T., Georgescu, G. N., Dului, O. G., & Szobotka, S. A. (2001). 3-D dual gamma-ray computer axial tomography investigation of polymetallic nodules. *Deep Sea Research Part I: Oceanographic Research Papers*, 48(11), 2529–2540.
- Schott, D., et al. (2021). esign framework for DEM-supported prototyping of grabs including full-scale validation. *Journal of Terramechanics*, 96, 29–43.
- Shook, C., Haas, D., Husband, W., & Small, M. (1979). *Degradation of coarse coal particles during hydraulic transport*. Kent, UK, 6th international conference on the hydraulic transport of solids in pipes.
- Spelay, R., Gillies, R., Hashemi, S., & Sanders, R. (2016). Effect of pipe inclination on the deposition velocity of settling slurries. *The Canadian Journal of Chemical Engineering*, 94(6), 1032–1039.
- Tavares, L. M. (2022). Review and further validation of a practical single-particle breakage model. *Kona Powder and Particle Journal*, 39, 62–83.
- van den Bergh, C., & Alvarez Grima, M. (2006). Tbilisi, Georgia, 13th international conference on transport and sedimentation of solid particles.
- van Wijk, J. (2016). *Vertical hydraulic transport for deep sea mining: A study into flow assurance*. TU Delft.
- van Wijk, J., & de Hoog, E. (2020). Size reduction of CCZ polymetallic nodules under repeated impact fragmentation. *Results in Engineering*, 7, 100154.
- van Wijk, J., Talmon, A., & van Rhee, C. (2016). Stability of vertical hydraulic transport processes for deep ocean mining: An experimental study. *Ocean Engineering*, 125, 203–213.
- van Wijk, J., et al. (2019). Impact fragmentation of polymetallic nodules under deep ocean pressure conditions. *Minerals Engineering*, 134, 250–260.
- Vlasak, P., Chara, Z., Konfirst, J., & Kysela, B. (2013). *Experimental investigation of coarse-grained particles in pipes*. Rostock, Germany, 16th international conference on the transport and sedimentation of solid particles.
- Worster, D., & Denny, D. (1955). *Hydraulic transport of solid material in pipes*. s.l., Proceedings of the Institution of Mechanical Engineers.
- Yamazaki, T., & Sharma, R. (2001). *Preliminary experiment on powderization of deep-sea sediment during hydraulic transport*. Poland, 4th ocean mining symposium.
- Yamazaki, T., Tsurusaki, K., & Handa, K., (1991). *Discharge from manganese nodule mining system*. Edinburgh, UK, First international offshore and polar engineering conference.



**Dingena Schott** is full professor of Machine Cargo Interaction Engineering at TU Delft's department of Maritime and Transport Technology. She obtained her PhD in 2004 from TU Delft on the homogenization of bulk materials in mammoth silos. She is fascinated by the complex behaviour of granular materials and the interaction with equipment operating in a logistic context. In 2007, she started the GranChaMlab@TUDelft to characterize, model, calibrate and validate granular materials for enabling simulation-supported design for cargo handling equipment on an industrial scale. Since then she has worked on developing calibration frameworks and modelling particle-based systems in various design contexts, including terminal designs for particulate materials, as well as an award-winning new grab design. Her main research interests include: machine-cargo interfaces, simulation-supported design, biomass materials and energy transition-driven handling and logistics.



**Edwin de Hoog** received his MSc in offshore and dredging technology from the Delft University of Technology in 2016. After that, Edwin started working as a research and development engineer at Royal IHC and a part-time PhD researcher at the Department of Maritime and Transport Technology, section of Dredging Engineering, Delft University of Technology. He specializes in hydraulic transport of sand, gravel and manganese nodules and works on many related aspects of deep-sea mining. He mainly worked on flow assurance issues in jumper hoses and vertical pipelines and degradation of manganese nodules during hydraulic transport, as part of the EU Blue Mining and Blue Nodules programmes. As part of his PhD research, he developed 1D CFD technology to simulate pump-pipeline systems and the effect of slurry dynamics and density wave amplification on flow assurance, applicable for deep-sea mining and dredging pipelines.



**Jort van Wijk** received his MSc and PhD from Delft University of Technology, where he specialized in offshore engineering. The subject of his PhD was flow assurance of vertical hydraulic transport for deep-sea mining applications. Jort started his career in 2008 at the corporate R&D department of Royal IHC, manufacturer of specialized offshore, dredging and mining vessels and equipment, where he worked in different specialist and managerial roles on dredging and (deep-sea) mining technology. He was closely involved in the EU FP7 Blue Mining programme and the EU H2020 Blue Nodules programme, two major research programmes aimed at developing knowledge and technology for deep-sea mining. After joining IQIP in 2020, his area of interest expanded to offshore geotechnics and soil-structure interaction problems for foundation installation. Next to this, as an independent consultant, Jort has a continued interest in deep-sea mining technology.



**Rudy Helmons** obtained his MSc in Mechanical engineering in 2011, after which he started as a research engineer at Royal IHC. He obtained his PhD ‘cum laude’ from TU Delft in 2017 on the topic of rock excavation in underwater conditions. After that, he started as an assistant professor in offshore and dredging engineering at TU Delft, and was Adjunct Associate Professor for deep-sea mining at NTNU from Feb 2020–Feb 2024. He is currently associate professor and focuses his research on the handling of solids in a marine environment, for example excavation, transport, separation and deposition. He is the project coordinator of various (deep) seabed mining research projects.